World Academy of Science, Engineering and Technology
International Journal of Mechanical and Mechatronics Engineering
Vol:11, No:5, 2017

Characterization of Extreme Low-Resolution Digital Encoder for Control System with Sinusoidal Reference Signal

Zhenyu Zhang, Qingbin Gao

***Abstract*—**Low-resolution digital encoder (LRDE) is commonly adopted as a position sensor in low-cost and resource-constraint applications. Traditionally, a digital encoder is modeled as a quantizer without considering the initial position of the LRDE. However, it cannot be applied to extreme LRDE for which stroke of angular motion is only a few times of resolution of the encoder. Besides, the actual angular motion is substantially distorted by this extreme LRDE so that the encoder reading does not faithfully represent the actual angular motion. This paper presents a modeling method for extreme LRDE by taking into account the initial position of the LRDE. For a control system with sinusoidal reference signal and extreme LRDE, this paper analyzes the characteristics of angular motion. Specifically, two descriptors of sinusoidal angular motion are studied, which essentially sheds light on the actual angular motion from extreme LRDE.

***Keywords*—**Low resolution digital encoder, resource-constraint control system, sinusoidal reference signal, servo motion control.

I. Introduction

INCREMENTAL optical encoders, also known as shaft encoders, are widely used for precision motion control systems. It is an electro-mechanical device that converts the angular position to an analog or digital code. High precision motion control relies critically on the resolution of encoders as the feedback sensor. However, measurement precision is limited by the manufacturing technology of the encoders. Although advances in encoder technology have greatly improved the scale grating on linear optical encoders, the trade-off between resolution and cost is unavoidable. In many applications where the cost limitations are very stringent, capabilities of sensing will be compromised. In this context, many researchers have been conducted to increase the resolution of the encoder without changing the sensor hardware. Interpolation method is proposed which uses soft techniques to further improve the encoder resolution by processing the analog encoder signals to derive the small intermediate positions [1]-[3]. One disadvantage of this method is that it requires an additional analog-to-digital converter and increases computational costs. Also, more accurate position information can be extracted from the digital optical encoder by extrapolating polynomial fitting through previous collected time stamps [4]. This method is effective based on the condition that the encoder reading at each time stamp is accurate. However, in a digital encoder, the mapping from the true position to the measured position at each time stamp varies, depending on the initial position of LRDE, which will be discussed later in detail.

When LRDE has to be used as a position sensor in the control system, it is usually modeled as quantizer [5]-[8]. The quantizer model treats the initial position of the LRDE (called offset angle in this paper) as fixed; specifically, the quantizer is an odd function and the first quantization step is generated when the angular position reaches half of the resolution of the encoder. It works fairly well when the actual stroke of the angular motion is comfortably large with regard to the resolution of the encoder, e.g. angular motion is 10 times as large as the resolution of the encoder. For extreme LRDE application (i.e. stroke is only a couple of times of resolution of encoder), a quantizer model cannot reveal the mechanism of LRDE. The offset angle, a random variable in encoder, should be taken into account for control applications with extreme LRDE, which would be detailed later.

Extreme LRDE introduces severe nonlinearity into servo control systems as a position sensor. For reference of a sinusoidal signal, the encoder can only generate very limited steps for each direction from which the actual angular motion cannot be inferred directly. For example, in the Ros-Drill micro-injection, it needs to achieve sinusoidal trajectory tracking with a desired amplitude of 0.2 degree and an encoder with the resolution of 0.09 degree [9]. This setting allows only four steps of encoder reading (i.e. two steps up and two steps down), which is regarded as the desired encoder readings. An adaptive control mechanism is introduced to serve this purpose [10]. However, given the desired encoder readings, we still do not know much information about the actual angular motion. Specifically, the two important descriptors of actual angular motion, namely amplitude and bias, cannot be determined. The main contribution of this paper is to shed light on the characteristics and dynamics of actual motion which can be inferred from encoder readings. That is, although extreme LRDE is not capable of faithfully representing the actual motion in the servo control system, more information about these two descriptors can still be extracted for better insight into actual motion.

The paper is organized as follows. In Section II, modeling of extreme LRDE is introduced by comparison with a quantizer. Also, the SIMULINK model with LRDE is

Z. Zhang is with the Servo Department, Western Digital Corporation, Irvine, CA 92614 USA (phone: (860)-617-3168, e-mail: Zhenyu.Zhang@wdc.com).

Q. Gao is with the Mechanical and Aerospace Engineering Department, California State University, Long Beach, CA 90840 USA (e-mail: Qingbin.Gao@csulb.edu).

presented, which would be used for simulation later. Section III presents the characteristics of descriptors for sinusoidal angular motion from both amplitude and bias perspectives. Finally, conclusions about characteristics of extreme LRDE are given.

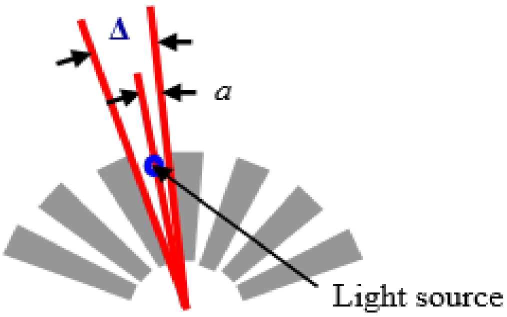

Fig. 1 Explanation of Encoder

II. Extreme LRDE in a Control System

A. Introduction of Offset Angle

Fig. 1 gives brief description of the principle of an optical incremental encoder, where Δ is the resolution of encoder. The small circle in Fig. 1 indicates the position of the light source. The angular position of encoder θ is defined as the absolute angular displacement of light source relative to the point in the disk which coincides with the position of the light source when the encoder is still. When the disk is still, $\theta = 0$ is named 'zero' position of θ.

We now present an argument on a crucial component of the extreme LRDE. Where a is the encoder offset angle, which is the angular motion needed for the first encoder pulse to register (see Fig. 1), "a" can be taken as a backlash dead-zone during which the encoder does not respond. Clearly it is an unknown and completely random quantity which is bounded, $0 < a < \Delta$, and its probability distribution is assumed to be uniform. That is, from the starting position $\theta = 0$, the encoder does not register any reading until $-a$ degree of rotation (in counterclockwise sense) or $\Delta - a$ degree (in clockwise sense) is completed (see Fig. 1). In Fig. 2, we further depict the sensing ability of the encoder on a hypothetical oscillation θ. Let us express θ as:

$$\theta = A_{12-b} + A\sin\omega(t - t_0) \tag{1a}$$

where $\omega = 2\pi f$ and A and f are amplitude and frequency of the harmonic wave, respectively, and t_0 is the initial time shift, as indicated in Fig. 2. The offset angle in encoder

$$0 < a < \Delta \tag{1b}$$

A_{12-b} is defined as the bias of the harmonic wave where, A_1 and A_2 are the upper and lower amplitude of θ, respectively and we have:

$$A_{12-b} = \frac{A_1 - A_2}{2} \tag{2}$$

Furthermore, we define the complete peak-to-peak stroke as $A_{12} = A_1 + A_2$ and we have $A_{12} = 2A$. A_{12} and A_{12-b} are two most important descriptors of sinusoidal angular motion.

In Fig. 2, the piece-wise continuous curve represents the rotational motion being sensed by the encoder and the encoder reading is denoted as θ_{enc}. The peak-to-peak angular stroke of θ_{enc} is named A_{enc}, which is 4Δ in Fig. 2.

The encoder can only trigger when θ reaches at angular displacements of $\Delta - a$, $2\Delta - a$, …, $m\Delta - a$ clockwise and $-a$, $-\Delta - a$, …, $-(m-1)\Delta - a$ counterclockwise, as indicated in Fig. 2. Therefore, the detection of the angular position may vary, i.e., the encoder may sense the same θ differently, depending on the encoder offset angle a.

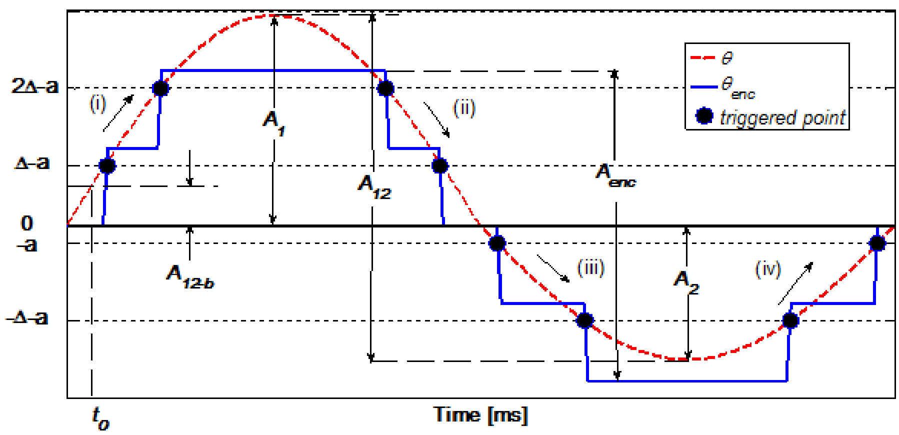

Fig. 2 Oscillation motion θ read by encoder; $0 < a < \Delta$ is the random offset angle)

B. Comparison of Extreme LRDE and Quantizer

The characteristics of a linear quantizer and that of extreme LRDE are shown in Figs. 3 (a) and (b), respectively. For both quantizer and encoder, for all continuous input θ, the output θ_{enc} can be only equal to discrete values 0, Δ, 2Δ, etc. However, the quantizer model triggers the first step when $\theta = \pm\Delta/2$ and the characteristic of the quantizer enjoys the property of odd symmetry with respect to origin; whereas, as described previously, the encoder model triggers the first step when $\theta = \Delta - a$ or $\theta = -a$, where $0 < a < \Delta$. If the resolution of the encoder is high compared to the total stroke, such an offset angle in the encoder would not cause a noticeable difference in sensing the motion, and we can use the quantizer to model an encoder with high resolution. However, if the resolution of the encoder is low compared to the stroke, the quantizer model cannot reveal the mechanism of the encoder and the offset angle in the encoder should be taken into account. In essence, the linear quantizer model is a special case for an encoder model in which $a = \Delta/2$. In the following analysis, this offset encoder will be taken into account to unveil the important characteristics of actual angular motion.

C. SIMULNK Model

The encoder model with the resolution Δ and offset angle a can be simulated in MATLAB/SIMULINK. To better explain the modeling of the encoder, the hypothetical oscillation (θ) in Fig. 2 is divided into four parts, labeled as (i), (ii), (iii) and (iv), respectively. They correspond to different portions of θ as follows:

$$\begin{array}{ll} (i) & \theta > 0 \;\; and \;\; \dot{\theta} > 0 \\ (ii) & \theta > 0 \;\; and \;\; \dot{\theta} < 0 \\ (iii) & \theta < 0 \;\; and \;\; \dot{\theta} < 0 \\ (iv) & \theta < 0 \;\; and \;\; \dot{\theta} > 0 \end{array} \tag{3}$$

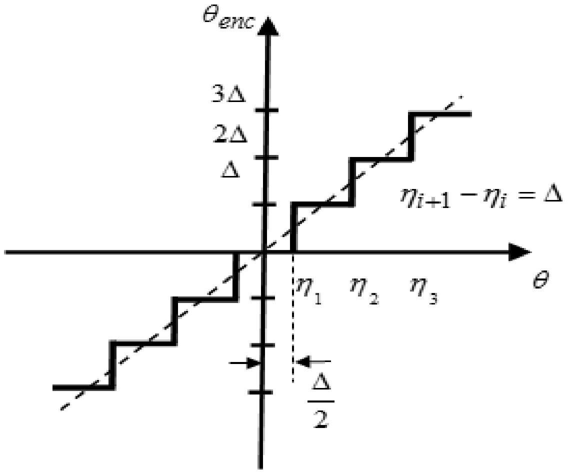

Fig. 3 (a) Linear quantizer characteristic

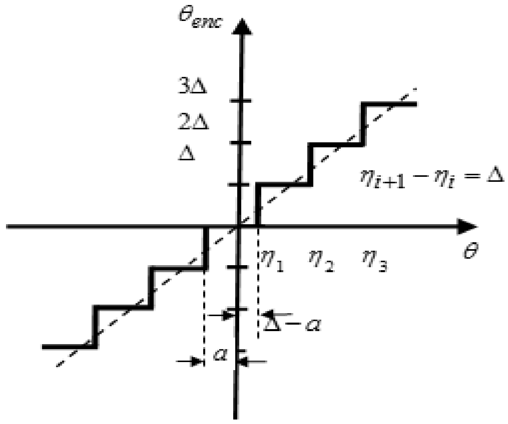

Fig. 3 (b) Encoder characteristic

Fig. 4 (a) shows the SIMULINK block for the encoder model. Four subsystems are built for detection of four different portions of θ and the output of each subsystem is times of being triggered, labeled as Out1, Out2, Out3 and Out4, respectively. The combination of these four outputs, labeled as 'Out' is the number of steps in the encoder, and hence, θ_{enc} can be obtained by multiplying the resolution of encoder (Δ) and 'Out', as indicated in Fig. 4 (a). Specifically, Fig. 4 (b) shows the SIMULINK block for the detection of part (i) of θ. It consists of logic operation blocks and counters, simulating each triggered condition of the encoder for part (i) of θ, depending on the initial angular offset, a as described in Fig. 2. The counter will count up by one once the condition of the logic operation is satisfied. The subsystems for others are similar except for the triggered conditions.

Fig. 5 shows the SIMULINK model for a typical position control system with PID control logic, which utilizes this encoder modeling method, where θ_d is the sinusoidal reference signal. The encoder block in Fig. 4 converts the continuous angular motion of the pipette, θ, into the discretization and holds it.

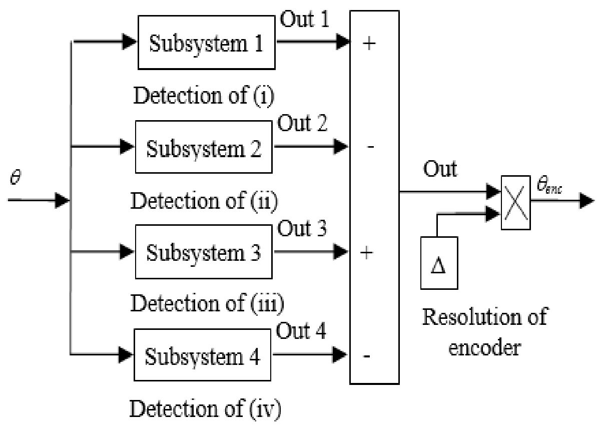

Fig. 4 (a) Encoder block

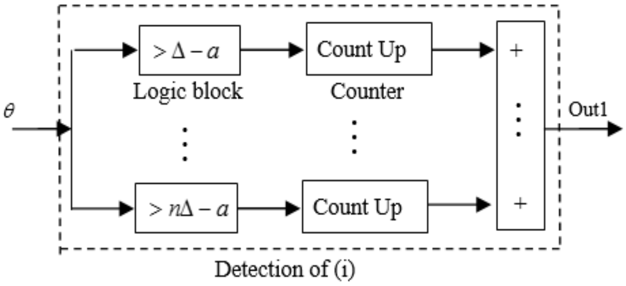

Fig. 4 (b) Simulation block for detection of (i)

The output of the encoder block, θ_{enc}, is the discretized reading of the angular motion by the encoder. The simulation result in the later section is conducted based on this platform.

III. Characteristics of Descriptors of Sinusoidal Angular Motion

For the servo control system with a sinusoidal reference signal, the integral effect in the control system can perform to have the encoder reading be symmetric with regard to zero position (see Fig. 2). That is, the number of steps in a positive and negative direction is the same. For example, in the Ros-Drill micro-injection application with desired a amplitude of 0.2 degrees and an encoder with a resolution of 0.09 degrees, it can achieve four steps of encoder reading (i.e. two steps up and two steps down) by an adaptive PID control mechanism [10]. The following section is devoted to analysis of the two descriptors after these desired encoder readings are achieved.

A. Reconstruction of Amplitude from Encoder Readings

A desired encoder readings to be $2n$-step peak-to-peak stroke, where n is 1, 2, ... can only guarantee actual peak-to-peak stroke of the shaft rotation to be between $(n-1)\Delta$ and $(n+1)\Delta$. For example, given the 4-step peak-to-peak stroke, actual stroke is not uniquely determined and instead it is randomly distributed with a relative stroke error between 0% and 32.5% (when $A_{12} = 3\Delta$) [9].

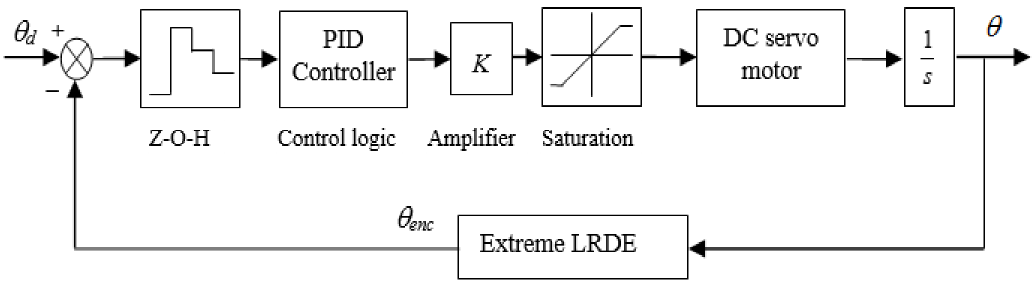

Fig. 5 SIMULINK model of the control system with extreme LRDE

It is found that some interesting features from the encoder reading can be extracted to determine actual peak-to-peak stroke of angular motion [11]. For the desired encoder reading of two steps up and down, the actual peak-to-peak stroke can be calculated as:

$$A_{12} = \frac{6\Delta}{\cos(\omega w_1) + \cos(\omega w_2)} \tag{4}$$

where $2w_1$ and $2w_2$ are the width of dwell time when θ_{enc} stays at peak encoder registrations, i.e. $2\Delta - a$ and $-\Delta - a$. Assuming we encounter 4Δ peak-to-peak stroke consistently, we can conjure up the corresponding A_{12}, which is un-measurable by simply observing the dwell periods at the peak encoder registrations, w_1 and w_2. This construction of amplitude from the encoder readings enables amplitude control with extreme LRDE. This formulation changes the treatment considerably, namely, we will simply monitor these two quantities at each cycle and implement a control law which will make them equal. Actual stroke is now uniquely determined from the encoder readings, which essentially converts the stochastic stroke control problem into a deterministic one.

B. Boundary of Bias

Bias is another important descriptor for sinusoidal angular motion. From Fig. 2, to have an encoder read $2n$ steps from peak-to-peak (i.e. $A_{enc} = 2n\Delta$), the following are the sufficient and necessary conditions of the upper amplitude (A_1) and lower amplitude (A_2). For A_1,

$$-a + n\Delta < A_1 < -a + (n+1)\Delta \tag{5a}$$

and for A_2,

$$a + (n-1)\Delta < A_2 < a + n\Delta \tag{5b}$$

by summing (5a) and (5b) we can obtain the necessary condition for $A_{enc} = 2n\Delta$,

$$(2n-1)\Delta < A_{12} < (2n+1)\Delta \tag{6}$$

or actual stroke (A_{12}), where $(2n-1)\Delta < A_{12} < (2n+1)\Delta$, A_{12} can be further expressed as:

$$\begin{cases} for\ (2n-1)\Delta < A_{12} < 2n\Delta & A_{12} = (2n-1)\Delta + \varepsilon \\ for\ 2n\Delta \le A_{12} < (2n+1)\Delta & A_{12} = (2n+1)\Delta - \varepsilon \end{cases} \tag{7}$$

where ε is the absolute deviation of A_{12} from its nearest odd integer multiple of Δ and $0 < \varepsilon < \Delta$. Furthermore, for the simplicity of expression, let us define $\overline{A_{12-b}}$ as:

$$\overline{A_{12-b}} = \frac{\Delta - 2a}{2} \tag{8}$$

Note that the offset angle is a uniformly distributed random variable between 0 and Δ. Hence, $\overline{A_{12-b}}$ is a uniformly distributed random variable between $-\Delta/2$ and $\Delta/2$.

Proposition 1: For a particular A_{12}, where $(2n-1)\Delta < A_{12} < (2n+1)\Delta$, if and only if the bias of the stroke (A_{12-b}) is in the area with the center of $\overline{A_{12-b}}$ and the radius of $\varepsilon/2$, i.e.

$$\overline{A_{12-b}} - \varepsilon/2 < A_{12-b} < \overline{A_{12-b}} + \varepsilon/2 \tag{9}$$

the encoder signal is symmetric in the number of steps and $A_{enc} = 2n\Delta$. Especially, if $A_{12-b} = \overline{A_{12-b}}$, for any stroke, where $(2n-1)\Delta < A_{12} < (2n+1)\Delta$, $A_{enc} = 2n\Delta$ regardless of the offset angle.

Proof: First, we prove the sufficiency condition. By substituting (2) and (8) into (9), (5a) and (5b) can be satisfied. Therefore, if (9) is satisfied, $A_{enc} = 2n\Delta$.

Next the necessity condition is proven. Without loss of generality, let us look at $(2n-1)\Delta < A_{12} < 2n\Delta$. By substituting (7) into (6a), we obtain:

$$n\Delta - a < A_1 < n\Delta - a + \varepsilon \tag{10a}$$

$$(n-1)\Delta + a < A_2 < (n-1)\Delta + a + \varepsilon \tag{10b}$$

from (10a) and (10b), (9) can be derived. Especially, if $A_{12-b} = \overline{A_{12-b}}$, we can express A_1 and A_2 in terms of A_{12}:

$$A_1 = (A_{12} + \Delta - 2a)/2 \tag{11a}$$

$$A_2 = (A_{12} - \Delta + 2a)/2 \tag{11b}$$

Substituting (11) into (6), we can find that the conditions of offset angle for $A_{enc} = 2n\Delta$ are automatically satisfied. This implies that if $A_{12-b} = \overline{A_{12-b}}$, for any A_{12}, where $(2n-1)\Delta < A_{12} < (2n+1)\Delta$, $A_{enc} = 2n\Delta$ regardless of the offset angle. Therefore $\overline{A_{12-b}}$ is considered as "ideal" bias of the stroke for a particular offset angle (a).

From (9) for $A_{enc} = 2n\Delta$, bias is confined to the boundary dictated by ideal bias and ε. And the closer A_{12} is to its nearest odd integer multiple of Δ, the larger area is A_{12-b} allowed to move. As indicated previously, accurate stroke control with extreme LRDE can be achieved by reconstruction of amplitude from encoder readings. From analysis of the boundary of bias, we can actually achieve bias boundary control by controlling stroke (A_{12}).

C. Dynamics of Bias

Now we obtain the boundary of bias given $A_{enc} = 2n\Delta$. We can further look into the dynamics of bias as follows:

Proposition 2: Bias oscillates around ideal bias as if a restoring force acts on it. Specifically, for $A_{enc} = 2n\Delta$, if and only if $A_{12-b} = \overline{A_{12-b}}$, encoder signal θ_{enc} does npt contain the restoring force; else if $A_{12-b} > \overline{A_{12-b}}$, its restoring force > 0; else $A_{12-b} < \overline{A_{12-b}}$, its restoring force < 0. Besides, absolute value of restoring force increases with distance of A_{12-b} away from $\overline{A_{12-b}}$.

Proof: Let us define E_b to measure the deviation of bias of stroke (A_{12-b}) from "ideal" bias of angular motion ($\overline{A_{12-b}}$). That is:

$$E_b = A_{12-b} - \overline{A_{12-b}} \tag{12a}$$

from (9) and (12a), we have:

$$-\varepsilon/2 < E_b < \varepsilon/2 \tag{12b}$$

For the simplicity of the following analysis, the equivalent encoder model is used which leads to the same θ_{enc} for sensing θ, and it is:

$$\theta = A \sin \omega t \tag{13a}$$

and the offset angle in encoder is:

$$a_{eq} = a + A_{12-b} \tag{13b}$$

by substituting (13b) and (8) into (12a), (12a) can be reduced to:

$$E_b = \frac{2a_{eq} - \Delta}{2} \tag{14}$$

Without loss of generality, let us use $n = 2$ as the example, namely encoder reads two steps up and two steps down. Let t_i, where $i = 1, ..., 8$ represents each triggered time instant in one cycle of θ, t_i can be obtained from (13a).

$$A\sin\omega t_i = \eta_i \tag{15}$$

where η_i corresponds to encoder values at time instant $i=1,2,5,6$ and they are $\Delta - a$, $2\Delta - a$, $-a$ and $-\Delta - a$ for $n=2$. From (15), we have:

$$t_i = \frac{\sin^{-1}(\frac{\eta_i}{A})}{\omega}, \text{ i=1,2,5,6} \tag{16a}$$

Due to the symmetry of θ with respect to $\omega t = \pi/2$ and $\omega t = 3\pi/2$, we have:

$$t_i = \frac{\pi}{\omega} - t_{2-floor(i-2.5)}, \text{ i = 3,4} \tag{16b}$$

$$t_i = \frac{3\pi}{\omega} - t_{6-floor(i-6.5)}, \text{ i = 7,8} \tag{16c}$$

One period of encoder reading from θ can be expressed as:

$$\theta_{enc} = \begin{cases} \Delta & t_i < t < t_{i+1} \; i=1,4 \\ 2\Delta & t_i < t < t_{i+1} \; i=2 \\ -\Delta & t_i < t < t_{i+1} \; i=5,7 \\ -2\Delta & t_i < t < t_{i+1} \; i=6 \\ 0 & others \end{cases} \tag{17}$$

Therefore, the magnitude of DC component of θ_{enc} can be expressed as:

$$c_0 = \frac{1}{T}\int_0^T \theta_{enc}(t)dt \tag{18}$$

by substituting (16) and (17) into (18), c_0 can be rewritten as

$$c_0(a_{eq}, A_{12}, \Delta) = \frac{1}{\pi}\sum_{i=1}^{N} \sin^{-1}(\frac{2\eta_i}{A_{12}}) \tag{19}$$

by applying (14) into (19) and knowing that $A_{12} = 2A$, c_0 can be expressed in terms of E_b,

$$c_0(E_b, A_{12}, \Delta) = \frac{1}{\pi}\sum_{i=1}^{N} \sin^{-1}(\frac{\lambda_i \Delta + 2E_b}{A_{12}}) \tag{20}$$

where $\lambda_i = 1, -1, 3, -3$. Note that $c_0(E_b, A_{12}, \Delta)$ is the odd symmetry with regard to E_b. From (20), we can find:

$$c_0(E_b, A_{12}, \Delta)\begin{cases} <0 & for\ -\varepsilon/2 < E_b < 0 \\ =0 & for \quad E_b = 0 \\ >0 & for\ 0 < E_b < \varepsilon/2 \end{cases} \tag{21a}$$

and,

$$\frac{\partial c_0(|E_b|, A_{12}, \Delta)}{\partial E_b} > 0 \tag{21b}$$

where $-\varepsilon/2 < E_b < \varepsilon/2$. From (21), it can be concluded that if $E_b = 0$ (i.e. $A_{12-b} = \overline{A_{12-b}}$), induced DC component in θ_{enc} is zero and its absolute value increases with the increasing of $|E_b|$. QED.

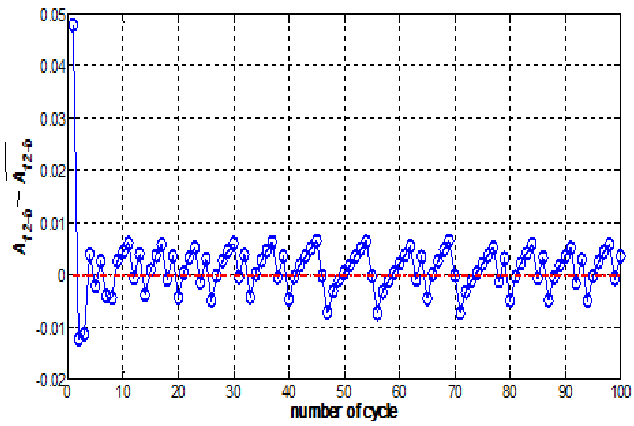

Fig. 6 Dynamics of A_{12-b} relative to $\overline{A_{12-b}}$ at $A_{enc} = 4\Delta$

In a negative feedback control system with sinusoidal reference signal, if θ_{enc} contains a DC component, due to negative feedback effect, the control signal fed into actuator contains a DC component but with opposite sign, pushing bias of stroke (A_{12-b}) of angular position towards its "ideal" position $\overline{A_{12-b}}$ by adjusting A_1 and A_2 value. Therefore it seems that feedback control serves as a restoring force acting on the A_{12-b}. In other words, feedback effect acts on A_{12-b} like a spring, having A_{12-b} approach "ideal" bias of stroke ($\overline{A_{12-b}}$).

Fig. 6 shows one simulation example of movement of bias from the position control system with extreme LRDE in Fig. 5. In this example, PID parameters are tuned to have $A_{enc} = 4\Delta$ at first. From Fig. 6, A_{12-b} oscillates around $\overline{A_{12-b}}$, validating the restoring effect on A_{12-b}; in this case, $A_{12} = 0.31$ and correspondingly, $\varepsilon/2 = 0.02$. In order to have $A_{enc} = 4\Delta$, A_{12-b} is allowed to move only within $(-0.02, 0.02)$ relative to $\overline{A_{12-b}}$. Since A_{12-b} does not move beyond this boundary, $A_{enc} = 4\Delta$ in this example, as observed in the simulation.

IV. Conclusions

Offset angle, a random variable between zero and the resolution of an encoder, differentiates a model of a low-resolution encoder from a quantizer. In this paper, the characteristics of a low-resolution encoder for sinusoidal trajectory tracking are described in detail. The amplitude and bias of the actual angular motion can be inferred from the encoder readings, which lead to a much better understanding of actual motion in a control application with an extreme low-resolution encoder. These capabilities enable stroke and bias control for a servo control system with extreme LRDE.

NOMENCLATURE

θ	Angular position of pipette holder (deg)
θ_{enc}	Angular position sensed by encoder (deg)
θ_d	Desired harmonic trajectory (deg)
A_d	Amplitude of θ_d (deg)
f_d	Frequency of θ_d (Hz)
Δ	Resolution of position sensor (deg)
a	Encoder offset angle (deg)
A_{12}	Peak-to-peak angular stroke of θ (deg)
$A_{12\text{-b}}$	Bias of θ (deg)
A_{enc}	Peak-to-peak angular stroke of θ_{enc} (deg)
$\overline{A_{12}}$	Average of A_{12} over some cycles (deg)
w_1(w_2)	Dwell time when θ_{enc} stays at extreme readings (s)
$\overline{A_{12-b}}$	Ideal bias of sinusoidal angular motion (deg)
ε	Deviation of A_{12} from its nearest odd integer multiple of Δ (deg)
η_i	Encoder values at triggering instant (deg)
E_b	Deviation of A_{12-b} from $\overline{A_{12-b}}$ (deg)
c_0	Magnitude of DC component of θ_{enc} (deg)

REFERENCES

[1] N. Hagiwara, Y. Suzuki, and H. Murase, “A method of improving the resolution and accuracy of rotary encoders using a code compensation technique,” IEEE Trans. Instrumentation and Measurement, vol. 41, no. I , pp. 98-101, Feb. 1992.

[2] K.K. Tan, H.X. Zhou, T.H. Lee, “New interpolation method for quadrature encoder signals,” IEEE Trans. Instrumentation and Measurement, 51 (2002), pp. 1073–1079.

[3] J. R. R. Mayer, “High resolution of rotary encoder analog quadrature signals,” IEEE Trans. Instrumentation and Measurement, vol. 43, no. 3, pp. 82–89, Jun.1994.

[4] T.A.C. Verschuren, “Extracting more accurate position and velocity estimations using time stamping”, Bachelor’s Thesis, Eindhoven, June 23, 2006.

[5] R.C. Kavanagh, J.M. Murphy, “The effects of quantization noise and sensor non-ideality on digital differentiator-bases rate measurement”, IEEE Trans. Instrumentation and Measurement, vol. 47, no. 6, pp. 1457–1463, Jun.1998.

[6] J. J. Abbott and A. M. Okamura, “Effects of position quantization and sampling rate on virtual-wall passivity”, IEEE Trans. Robotics, vol. 21, no. 5, pp.952 - 964 , 2005.

[7] Diolaiti, N., Niemeyer, G., Barbagli, F. and Salisbury, K. (2006), “Stability of haptic rendering: quantization, discretization, time-delay and Coulomb effects,” IEEE Transactions on Robotics, vol. 22, no. 2, pp. 256–268, 2006.

[8] Renat Iskakov, etc, “Influence of sensor quantization on the control performance of robotics actuators.” Proceedings of the 2007 IEEE/RSJ International Conference on Intelligent Robots and Systems, San Diego, CA, USA, Oct 29 - Nov 2, 2007.

[9] Z. Zhang and N. Olgac, An Adaptive Control Method for Ros-Drill cellular Microinjector with Low-resolution Encoder, Journal of Medical Engineering, vol. 2013, Article ID 418068, 11 pages, 2013.

[10] Z. Zhang and N. Olgac, Adaptive Gain Scheduling for Rotationally Oscillating Drill (Ros-Drill), with Low-Resolution Feedback, International Journal of Mechatronics and Manufacturing Systems, vol. 6, Nos. 5/6, 2013.

[11] Z. Zhang, N. Olgac and Q. Gao, An Effective Algorithm to Achieve Accurate Sinusoidal Amplitude Control with an Extremely Low-resolution Encoder, Advanced Intelligent Mechatronics, 2017, submitted for publication.